Growth and characterization of $Fe_{0.82}Ni_{0.18}$/V(001) superlattices

2003 J. Phys.: Condens. Matter 15 625

(http://iopscience.iop.org/0953-8984/15/4/303)

INSTITUTE OF PHYSICS PUBLISHING JOURNAL OF PHYSICS: CONDENSED MATTER

J. Phys.: Condens. Matter **15** (2003) 625–633 PII: S0953-8984(03)55203-1

Growth and characterization of $Fe_{0.82}Ni_{0.18}$/V(001) superlattices

A M Blixt[1], G Andersson[1,3], J Lu[2] and B Hjörvarsson[2]

[1] Department of Physics, Uppsala University, Box 530, SE-751 21 Uppsala, Sweden
[2] Department of Materials Science, Uppsala University, Box 534, SE-751 21 Uppsala, Sweden

E-mail: gabriella.andersson@fysik.uu.se

Received 24 October 2002
Published 20 January 2003
Online at stacks.iop.org/JPhysCM/15/625

Abstract

Epitaxial $Fe_{0.82}Ni_{0.18}$/V(001) superlattices grown by dc magnetron sputtering on MgO(001) substrate were investigated structurally by means of x-ray diffraction, Rutherford backscattering spectrometry and transmission electron microscopy. The results show that samples grown around 150 °C have high interface sharpness with low interdiffusion and good crystallographic quality.

1. Introduction

Sputter growth of magnetic multilayers/superlattices (SL)[4] has been used extensively in order to explore the magnetic properties for certain material and substrate combinations [1]. For example, the interlayer exchange coupling (IEC) between the ferromagnetic layers separated by a non-ferromagnetic spacer can be substantially affected by the growth mode through introduced strain, etc [2].

The strain induced by the lattice mismatch between the constituents in a multilayer/superlattice is related to the growth mode as describe in e.g. the force balance theory of Matthews and Blakeslee [3, 4]. Below a critical thickness the film is strained by the substrate lattice, and coherent, pseudomorphic interfaces are formed between the two metals with the same in-plane lattice parameter. Above the critical thickness the strain is relaxed by the introduction of misfit dislocations, which results in incoherent interfaces. In Fe/V(001) SL the lattice mismatch between Fe and V is rather large (5%), and experiments have shown that the growth becomes incoherent around 15–16 monolayers (ML) of V [5]. An incoherent growth reduces the spin-dependent electron reflection at the interfaces, which complicates the study of the oscillatory IEC postulated by theory [6].

In order to change the growth mode we have introduced a substitutional FeNi alloy with 19 wt% (18 at.%) of nickel. This alloy composition has a bcc structure, and is thus below

[3] Author to whom any correspondence should be addressed.
[4] A multilayer is an artificial structure with layers of different materials deposited on top of each other and repeated several times. A superlattice is a multilayer with a high in-plane and out-of-plane crystal coherence.

the phase transition into the fcc Invar region. Tang and co-workers [7] have investigated the structural and magnetic properties of $Fe_{1-x}Ni_x$/Cu SLs ($x = 0.2$–0.54). They found a complex morphology for the $Fe_{0.8}Ni_{0.2}$/Cu sample, with a few ML of bcc-like Fe–Ni crystallites formed epitaxially on top of the first Cu sublayer, and the rest of the sample grown in a more polycrystalline manner, i.e. by Stranski–Krastanov growth. No other investigations on multilayers or SL involving bcc Fe–Ni alloys exist to our knowledge.

In this paper we report the results of growing multilayers of $Fe_{0.82}Ni_{0.18}$/V on MgO(001) substrates at different temperatures and compare the structural quality with the Fe/V SL. The alloying will also change the Fe magnetic moment and the anisotropy. This together with the growth mode will have an influence upon the IEC, as will be reported in a forthcoming paper [8].

2. Experimental details

2.1. Growth

All samples were grown on one-side-polished MgO(001) substrates by dc magnetron sputtering in a UHV chamber. For a more detailed description of the system, see [5]. The substrates of dimension $10 \times 10 \times 0.5$ mm^3 were annealed at approximately 625 °C in UHV (10^{-10} Torr) for 10 min. Thereafter they were kept at the growth temperature for at least 25 min prior to film growth. The FeNi target with 19 wt% of Ni has a purity of 99.95% and the V target has a purity of 99.7%. Hereafter we will use the abbreviation FeNi instead of $Fe_{0.82}Ni_{0.18}$.

A series of films with 25 repetitions of the nominal bilayer composition [FeNi(15 Å)/V(15 Å)] were made with different substrate temperatures in the range 100–400 °C. The deposition rate for FeNi was 0.6 Å s^{-1} and the deposition rate for V was 0.4 Å s^{-1}. The sputter gas (Ar) pressure was 5.0 mTorr for the first 11 samples, and the substrate was kept at a floating potential. Additional samples were grown at the most favourable temperature and at slightly higher argon pressures (7.0 and 10.0 mTorr), which results in a lower kinetic energy of the sputtered particles impinging on the substrate, thereby reducing the deposition rates slightly. The V plasma could not be sustained at pressures below 5.0 mTorr.

2.2. Structural and compositional characterization

The structural quality of the films was investigated with low- and high-angle XRD using x-rays from a Cu K_α source in a conventional focusing Bragg–Brentano set-up (Siemens/Bruker D5000). The beam was defined by 0.3° divergence and receiving slits. The low-angle scans were performed from 0.5° up to 18° in 2θ with a step size of 0.01°, and the high-angle scans were performed in the region $2\theta = 45°$–$80°$ with a step size of 0.04°.

In order to deduce the film texture, {110} pole scans of some samples were performed by a full rotation around the out-of-plane axis, Φ, and with a tilt of the sample, Ψ (texture scan). A Philips X'Pert MRD set-up was used with a point focus Cu Kα x-ray source operating with a capillary lens together with crossed slits (8×8 mm^2) as the incident beam optics. The diffracted beam optics consisted of a 0.27° parallel plate collimator and a monochromator before a solid-state detector. The same machine was used with line focus and mirror optics for the two-dimensional reciprocal-space mapping (RSM) around the SL(002), (112), and (022) Bragg peaks.

The composition of a sputter-deposited film tends to be the same as that of the target if certain criteria are fulfilled. In our case, the film composition was investigated by RBS (Rutherford backscattering spectrometry) [9]. The combined nuclear scattering and energy

loss of the impinging particles (2 MeV He^+) can be simulated to yield a composition depth profile, in terms of surface densities of the masses in the superlattice, by a computer program such as RUMP [10].

The surface structure was investigated *in situ* using RHEED (reflection high-energy electron diffraction). Images were taken of the diffraction pattern seen on the fluorescent screen with the electron gun operating at 10 kV and a filament current of 3.5 A.

One FeNi/V sample was characterized by transmission electron microscopy (TEM). A cross-section specimen was made by gluing two pieces of the thin-film sample face to face and subsequently cutting slices of the sandwich. Each slice constituted a cross-section which was mechanically ground on both sides to a final thickness of 100 μm. The cross-section was thereafter dimpled down to a thickness of 10 μm at the specimen centre. The final thinning step was ion milling to electron transparency. The analysis was carried out using both a Tecnai F30 ST field emission gun TEM operated at 300 kV with a Gatan imaging filter and a Jeol 2000 FXII TEM operated at 200 kV.

3. Results and discussion

The D5000 reflectivity (low-angle) and high-angle XRD scans on FeNi/V(001) SL grown at different temperatures at 5 mTorr are shown in figure 1. From simulation of the reflectivity scans using the Philips simulation program WinGixa [11, 12], the bilayer thickness was deduced to be slightly higher than the nominal one, around 33.7 Å, with individual layer thicknesses of $\sim$11 and 12 ML (1 ML $\approx$ 1.45 Å) for the FeNi and the V layer, respectively.

The optimized substrate temperature was deduced to be around 150 °C at an argon pressure of 5 mTorr. This temperature is highly reduced compared to the optimized temperature for the pure Fe/V superlattice with a much more narrow temperature window around 300 °C [5]. Argon pressures higher than 5 mTorr did not improve the structural quality.

The quality of the film was deduced from the oscillations due to the superlattice period (chemical modulation), as well as the number of satellites in the high-angle region. The number of satellites is a measure of how well defined the repeat distance of the bilayers is, assuming coherence between successive layers. This assumption will be shown below to be correct. The thin-film thickness oscillations (Kiessig fringes) are seen up to 9.5° in 2θ, indicating a small total thickness variation. The high-angle XRD data shows the fundamental (002) Bragg peak of the film with three (two) satellite peaks in the lower-angle (higher-angle) range. The asymmetry between the intensity of the satellites above and below the Bragg peak angle is due to biaxial strain in the film [13].

The measured reflectivity of a sample grown at 150 °C was simulated with WinGixa. In the simulation program, the interface roughness is estimated by the root mean square deviation of the position of an interface atom in a perfectly smooth interface (the Fresnel coefficients are multiplied by a Debye–Waller-like factor). The experimental data are shown in figure 2 together with a simulation obtained using an interface roughness of 2.1 Å. This interface width is similar to that of the Fe/V(001) SL [5].

The pole figure, measured in the Philips MRD, of the {110} SL peaks for a sample grown at 150 °C shown in figure 3 clearly illustrates a fourfold symmetry as expected for a (001)-oriented bcc structure. In all the measured samples, the superlattice {110} peaks are rotated by 45° relative to the {220} peaks of the substrate. This rotational epitaxial relationship (FeNi/V(001) $\parallel$ MgO(001), FeNi/V[110] $\parallel$ MgO[010]) has previously been seen for the Fe/V(001) SL [5]. Taking this together with the high-angle XRD, we can confirm epitaxial growth of the superlattice films independent of the substrate temperature between 100 and 400 °C.

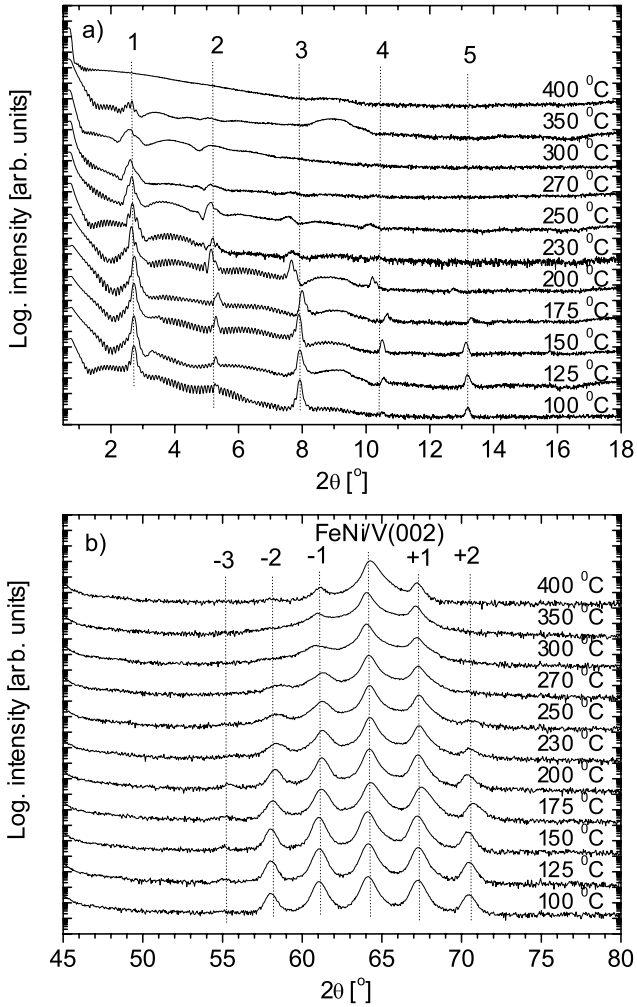

Figure 1. (a) Experimental x-ray reflectivity and (b) high-angle XRD curves for FeNi(11 ML)/V(12 ML) samples grown at different temperatures T at 5.0 mTorr. The peak numbers shown indicate the order of the superlattice peaks. The scans are shifted for clarity.

Reciprocal-space maps, also measured in the Philips MRD, around the SL(002) and (112) Bragg peaks are presented in figure 4 for a sample grown at the optimized substrate temperature (150 °C). The intensity of the XRD is mapped out in the in-plane (x-axis) and out-of-plane (y-axis) directions of the sample surface. The axes are in the dimensionless reciprocal-lattice units given in the software, which are the scattering vectors, Q_x and Q_y, times half the wavelength, $\lambda/2$.

The angular spread of the mosaic blocks is estimated to be around 0.9° from the full width at half-maximum (FWHM) of the rocking curve (ω-scan) on the SL(002) peak. This can be compared to the FWHM of the rocking curve on the MgO(002) peak, which was 0.03°. Also, two domains of the substrate were revealed. The crystalline coherence length, i.e. the distance over which the positions of the atoms are quantitatively correlated, projected either in-plane

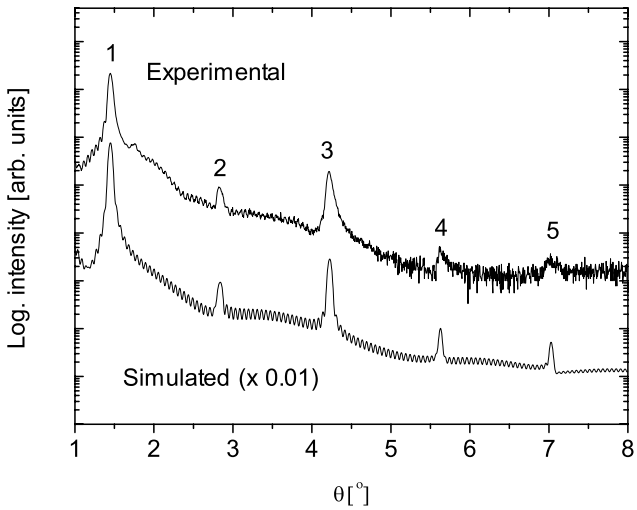

Figure 2. Experimental and simulated x-ray reflectivity (shifted for clarity) curves of a FeNi/V sample grown at 150 °C. The peak numbers shown indicate the order of the superlattice peaks. The scans are shifted for clarity. The total reflection edge is omitted due to saturation of the detector.

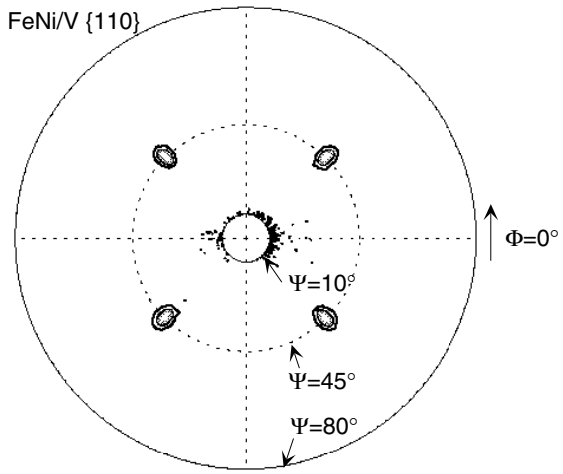

Figure 3. The pole figure of the FeNi/V{110} peaks from the sample grown at 150 °C presented in a Wulff projection. The sample is tilted an angle, Ψ, between 10° and 80°. The maximum intensity in the iso-intensity contours is 250 000 counts, whereas all intensity below 250 counts is suppressed. The MgO{220} peaks (not shown) occur at $\Phi = 0$, 90, 180, and 270°.

or out-of-plane, can be calculated using [14, 15]:

$$\xi = \frac{2\pi}{Q \cdot \mathrm{FWHM}^{\mathrm{rad}}}, \tag{1}$$

where ξ is the crystalline coherence length, Q is the scattering vector and the Bragg reflection's $\mathrm{FWHM}^{\mathrm{rad}}$ is given in radians.

In the out-of-plane direction (θ–2θ scans), the FWHM of the FeNi/V(002) peak is approximately 0.3°, resulting in a coherence length of about 270 Å, which is 1/3 of the total SL thickness. This is confirmed by the out-of-plane projections of the FeNi/V peaks (112) and

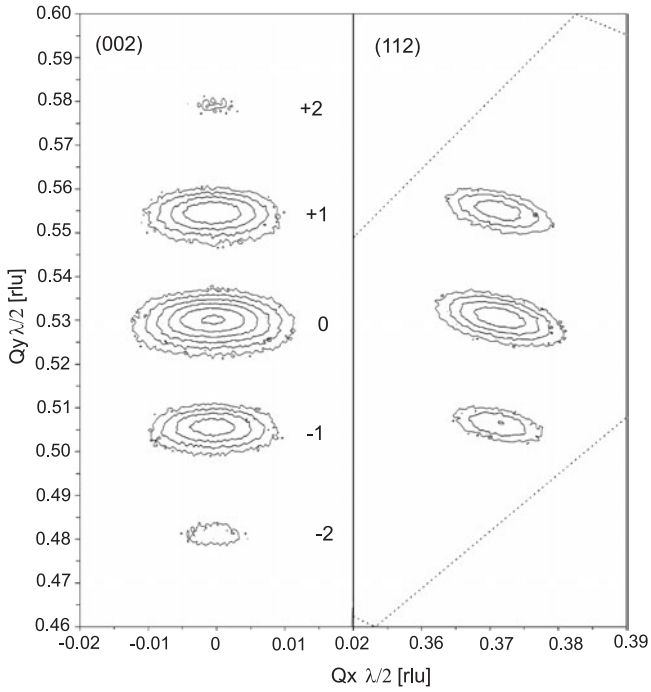

Figure 4. Reciprocal-space maps from the regions around the (002) and (112) Bragg peaks of the FeNi(11 ML)/V(12 ML) sample grown at 150 °C. Q_x and Q_y are the scattering vectors in the in-plane and out-of-plane directions of the sample, respectively. The numbers in the figure indicate the orders of the satellites. The iso-intensity contours are at 50, 100, 200, 400, 800 and 1600 counts s^{-1}, respectively.

(022). The in-plane coherence length was estimated to be 160 and 120 Å in the [110] and [020] directions, respectively. The values of the coherence lengths are considered to be lower limits since no consideration is taken of the broadening due to the lateral and longitudinal coherence lengths of the x-ray source, specimen curvature, and inhomogeneous strains in the film. The FWHM of the substrate (002) Bragg peak was at most 0.1°.

In comparison with the case of the similar Fe/V SL, the mosaicity is larger by more than a factor of 4, whereas the out-of-plane and the in-plane crystal coherence lengths are reduced by more than a factor of 2 and 3, respectively [5]. Still, since the crystal coherence lengths are much larger than the bilayer thickness, the film can be considered to have a superlattice structure. Thus one is justified to judge the structural quality by the number of satellites in the x-ray reflectivity and diffraction data.

From the RSMs of the SL(002), (112) and (022) peaks the average out-of-plane and in-plane lattice parameters, c and a, were estimated to be 2.904(5) and 2.937(5) Å, respectively, assuming a tetragonal distortion of the lattice (bct structure). The in-plane lattice spacing of the MgO [110] direction is $4.213/\sqrt{2} = 2.979$ Å showing that the film is adjusting to the substrate with a lattice mismatch of -1.4%. Assuming that the film is strained with the same in-plane lattice parameter throughout the film, the V lattice is biaxially compressed in the plane by 2.7% and the FeNi lattice is biaxially expanded by 2.3% compared to their bulk values.

The individual out-of-plane lattice parameters, c_i, were estimated from [16]

$$c_i = a_0\left(1 - \varepsilon_{\parallel}\frac{2\nu_i}{1-\nu_i}\right), \tag{2}$$

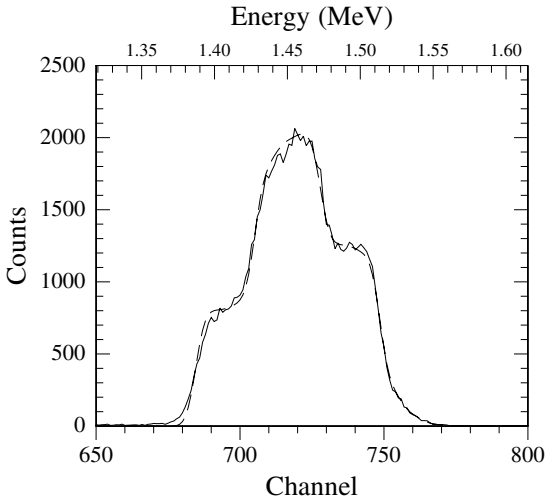

Figure 5. Part of the Rutherford backscattering spectrum of 2.0 MeV He^+ ions together with the simulation (dashed curve) of the FeNi/V(001) superlattice sample grown at 150 °C. The angle of incidence was 6°.

where a_0 is the unstrained lattice parameter, $\varepsilon_\parallel$ is the in-plane strain, and ν_i is Poisson's ratio for i = V or FeNi.

Equation (2) results in out-of-plane lattice parameters of $c_V = 3.106$ Å and $c_{FeNi} = 2.792$ Å, which corresponds to an expansion of 2.8% for the V lattice and a compression of 2.7% for the FeNi lattice as compared to their bulk values.

The unstrained cubic lattice parameters $a_{0V} = 3.02$ Å and $a_{0Fe} = 2.87$ Å [17] and the Poisson ratios $\nu_V = 0.342$ and $\nu_{Fe} = 0.367$ [18] were used in the calculations. In [19] the lattice parameter at room temperature for bcc $Fe_{1-x}Ni_x$ bulk alloy is given up to $x = 0.05$. By extrapolating to our composition ($x = 0.18$), we find that the lattice parameter is similar to that of bulk Fe, which is confirmed by measurements made on a 1000 Å thick FeNi film ($c = 2.870(5)$ Å).

All XRD data show that there is no twinning present in these samples, which in principle could occur with (112) as the twinning plane since the overall structure is bcc. However, any twins would be visible as additional features in the results of the structural investigations.

From the RBS analysis the chemical composition of Fe and Ni in the alloy was confirmed within an estimated error of 2% (see figure 5). These measurements were performed in an absolutely calibrated scattering chamber, using corrected values of the stopping power deduced from analysis of samples with known composition. The fit was done both for 6° and 9° angle of incidence.

A sample grown at 150 °C was also investigated *in situ* by means of RHEED. A pattern of narrow streaks was observed. The streaks occur due to energy and angular spread of the beam and sample surface disorder, but the fact that the streaks are narrow indicates a small roughness. A weak intensity difference observed along the streaks could be due to short-range in-plane surface order. Overall, the RHEED observations indicate layer-by-layer growth of large crystals.

In addition, the microstructure of a sample grown at 150 °C was characterized by TEM. The periodicity and distinct multilayer structure are confirmed by the selected-area electron diffraction (SAED) pattern shown in the top of figure 6, where superlattice reflections are seen

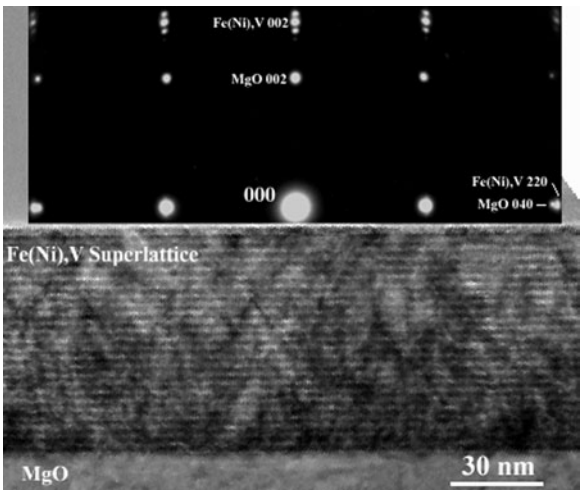

Figure 6. A cross-sectional TEM image of a FeNi/V(001) superlattice sample grown at 150 °C. The SAED pattern (top) is along the FeNi/V [1$\bar{1}$0] zone axis. Below that is a bright-field image acquired off the zone axis with the interface parallel to the electron beam.

near the FeNi/V(002) diffraction spot. These arise from the chemical modulation, just like the satellites in high-angle XRD, and thus give the same information. The epitaxial relationship between film and substrate can be obtained from the SAED pattern with FeNi/V(001) ‖ MgO(001), FeNi/V[110] ‖ MgO[010], which agrees with the XRD result. The epitaxial relationship has also been seen for a 1000 Å thick $Fe_{0.8}Ni_{0.2}$ film grown on MgO(001) [20]. Moreover, from the SAED pattern, which clearly shows the aforementioned mismatch between substrate and superlattice, the in-plane lattice parameter, a, is determined as 2.927 Å, which is in good agreement with the value obtained from the x-ray analysis (2.937 Å).

As discussed in the previous section, the film is strained, introducing diffraction contrast in the image, especially at the Bragg diffraction condition [21]. Therefore, to depress the stress effect and enhance the contrast, the image shown at the bottom of figure 6 was acquired slightly tilted from the Bragg diffraction condition while keeping the FeNi/V(002) plane parallel to the incident electron beam. The FeNi/V multilayer structure and the interfaces between the film and MgO substrate are clearly distinguished. There are fewer defects and less column-like growth in the FeNi/V superlattice as compared to the previously investigated Fe/V superlattice [22]. However, that specific sample had an interface roughness of ∼3 Å showing a deteriorated structural quality compared to the sample investigated in [5].

None of the methods used are able to resolve the Fe atom from the Ni atom; hence we do not know whether there is any surface segregation within the FeNi alloy layer. A surface segregation would affect the lattice matching between the magnetic and non-magnetic layer as well as the IEC. In the fcc phase, Schumann and co-workers [23], found the Ni segregation to be less than 5% for the $Fe_{1-x}Ni_x$ alloy. In the future, the bcc FeNi structure will be investigated by means of extended x-ray absorption fine structure (EXAFS).

4. Conclusions

A series of $Fe_{0.82}Ni_{0.18}$/V SL have been grown on MgO(001) at different temperatures. The overall structural quality is optimal for a temperature around 150 °C, as seen by investigations

done by means of low- and high-angle XRD. However, the crystalline quality improves at temperatures above 150 °C, at the cost of less sharp interfaces, since interdiffusion increases dramatically with rising substrate temperature. In comparison with the well-established case for Fe/V(001) SL, the mosaicity and the crystalline coherence length are reduced, whereas the interface widths are similar. The origin of this change could be the lower optimized growth temperature compared to that in the Fe/V case. The good crystal quality is confirmed by RHEED and TEM results, from which we could also deduce fewer defects and less column-like growth in the FeNi/V structure than the Fe/V structure. However, the Fe/V film studied by TEM in [22] had a larger interface width than the film previously studied in [5]. The FeNi composition is confirmed by means of RBS, while the possible surface segregation within the FeNi alloy layer is still an open question.

Acknowledgments

This work was carried out with financial support from the Swedish Foundation for Strategic Research (SSF) and the Royal Swedish Academy of Sciences (KVA).

References

[1] Schuller I K, Kim S and Leighton C 1999 *J. Magn. Magn. Mater.* **200** 571
[2] Hjörvarsson B, Dura J A, Isberg P, Watanabe T, Udovic T J, Andersson G and Majkrzak C F 1997 *Phys. Rev. Lett.* **79** 901
[3] Matthews J W, Blakeslee A E and Mader S 1976 *Thin Solid Films* **33** 253
[4] Matthews J W and Blakeslee A E 1976 *J. Cryst. Growth* **32** 265
[5] Isberg P, Hjörvarsson B, Wäppling R, Svedberg E B and Hultman L 1997 *Vacuum* **48** 483
[6] van Schilfgaarde M and Herman F 1993 *Phys. Rev. Lett.* **71** 1923
[7] Tang W, Gerhards Ch, Heise J and Zabel H 1996 *J. Appl. Phys.* **80** 2327
[8] Andersson G, Blixt A M, Stanciu V, Skubic B, Holmström E and Nordblad P 2003 *J. Magn. Magn. Mater.* submitted
[9] Baglin J E E and Williams J S 1989 *Ion Beams for Material Analysis* ed J R Bird and J S Williams (Sydney: Academic)
[10] www.genplot.com
[11] Parratt L G 1954 *Phys. Rev.* **95** 359
[12] de Boer D K G 1991 *Phys. Rev.* B **44** 498
[13] Guinier A 1963 *X-Ray Diffraction in Crystals, Imperfect Crystals and Amorphous Bodies* ed P Lorrain and D S-M Lorrain (San Francisco, CA: Freeman) p 279
[14] Cullity B D 1978 *Elements of X-ray Diffraction* (London: Addison-Wesley) p 102
[15] Granberg P, Isberg P, Svedberg E B, Hjörvarsson B, Nordblad P and Wäppling R 1998 *J. Magn. Magn. Mater.* **186** 154
[16] Birch J, Sundgren J-E and Fewster P F 1995 *J. Appl. Phys.* **78** 6562
[17] Ashcroft N W and Mermin N D 1976 *Solid State Physics* (Fort Worth, FL: Saunders) p 70
[18] Simmons G and Wang H 1971 *Single Crystal Elastic Constants and Calculated Aggregate Properties: A Handbook* vol 35 (Cambridge, MA: MIT Press) p 107
[19] Bonnenberg D, Hempel K A and Wijn H P J 1986 *Alloys Between 3d Elements (Landolt–Börnstein New Series)* Group III, vol 19a ed H P J Wijn (Berlin: Springer) p 148
[20] Yang J, Barna A, Makihara K, Hashimoto M and Barna P B 1999 *Thin Solid Films* **347** 85
[21] Sun H P, Zhang Z, Wang W D, Jiang H W and Lai W Y 2000 *J. Appl. Phys.* **87** 2835
[22] Broddefalk A, Mathieu R, Nordblad P, Blomqvist P, Wäppling R, Lu J and Olsson E 2002 *Phys. Rev.* B **65** 214430
[23] Schumann F O, Wu S Z, Mankey G J and Willis R F 1997 *Phys. Rev.* B **56** 2668